

## Changing water availability during the African maize-growing season, 1979–2010

This content has been downloaded from IOPscience. Please scroll down to see the full text.

2014 Environ. Res. Lett. 9 075005

(<http://iopscience.iop.org/1748-9326/9/7/075005>)

View [the table of contents for this issue](#), or go to the [journal homepage](#) for more

Download details:

IP Address: 128.112.33.188

This content was downloaded on 27/06/2017 at 16:07

Please note that [terms and conditions apply](#).

You may also be interested in:

[Robust features of future climate change impacts on sorghum yields in West Africa](#)

B Sultan, K Guan, M Kouressy et al.

[Water resources transfers through southern African food trade: water efficiency and climate signals](#)

Carole Dalin and Declan Conway

[A climatic deconstruction of recent drought trends in the United States](#)

Darren L Ficklin, Justin T Maxwell, Sally L Letsinger et al.

[The supply and demand of net primary production in the Sahel](#)

A M Abdi, J Seaquist, D E Tenenbaum et al.

[Uncertainty in future irrigation water demand and risk of crop failure for maize in Europe](#)

Heidi Webber, Thomas Gaiser, Roelof Oomen et al.

[Global warming induced hybrid rainy seasons in the Sahel](#)

Seyni Salack, Cornelia Klein, Alessandra Giannini et al.

[Drought effects on US maize and soybean production: spatiotemporal patterns and historical changes](#)

Samuel C Zipper, Jiangxiao Qiu and Christopher J Kucharik

[Projections of rapidly rising surface temperatures over Africa under low mitigation](#)

Francois Engelbrecht, Jimmy Adegoke, Mary-Jane Bopape et al.

[Darfur: rainfall and conflict](#)

Michael Kevane and Leslie Gray

# Changing water availability during the African maize-growing season, 1979–2010

Lyndon D Estes<sup>1,2</sup>, Nathaniel W Chaney<sup>2</sup>, Julio Herrera-Estrada<sup>2</sup>, Justin Sheffield<sup>2</sup>, Kelly K Caylor<sup>2</sup> and Eric F Wood<sup>2</sup>

<sup>1</sup> Woodrow Wilson School, Princeton University, Princeton, NJ 08544, USA

<sup>2</sup> Civil and Environmental Engineering, Princeton University, Princeton, NJ 08544, USA

E-mail: [lestes@princeton.edu](mailto:lestes@princeton.edu)


Received 20 December 2013, revised 11 June 2014

Accepted for publication 12 June 2014

Published 11 July 2014

## Abstract

Understanding how global change is impacting African agriculture requires a full physical accounting of water supply and demand, but accurate, gridded data on key drivers (e.g., humidity) are generally unavailable. We used a new bias-corrected meteorological dataset to analyze changes in precipitation (supply), potential evapotranspiration ( $E_p$ , demand), and water availability (expressed as the ratio  $P/E_p$ ) in 20 countries (focusing on their maize-growing regions and seasons), between 1979 and 2010, and the factors driving changes in  $E_p$ . Maize-growing areas in Southern Africa, particularly South Africa, benefitted from increased water availability due in large part to demand declines driven primarily by declining net radiation, increasing vapor pressure, and falling temperatures (with no effect from changing windspeed), with smaller increases in supply. Sahelian zone countries in West Africa, as well as Ethiopia in East Africa, had strong increases in availability driven primarily by rainfall rebounding from the long-term Sahelian droughts, with little change or small reductions in demand. However, intra-seasonal supply variability generally increased in West and East Africa. Across all three regions, declining net radiation contributed downwards pressure on demand, generally over-riding upwards pressure caused by increasing temperatures, the regional effects of which were largest in East Africa. A small number of countries, mostly in or near East Africa (Tanzania and Malawi) experienced declines in water availability primarily due to decreased rainfall, but exacerbated by increasing demand. Much of the reduced water availability in East Africa occurred during the more sensitive middle part of the maize-growing season, suggesting negative consequences for maize production.

 Online supplementary data available from [stacks.iop.org/erl/9/075005/mmedia](http://stacks.iop.org/erl/9/075005/mmedia)


Keywords: water supply, water demand, trends, maize, sub-Saharan Africa

## 1. Introduction

African economies are heavily reliant on rain-fed, small-scale agriculture [1, 2], and this dependence is likely to increase as new lands are cleared to meet growing global food demand [3]. A large proportion of African farmland occurs in ‘drylands’ characterized by strongly seasonal rainfall that is

highly variable both within and between seasons [1, 2, 4]. This highly uneven and erratic precipitation is a key source of vulnerability for agricultural livelihoods [2, 5, 6], which is increasing and projected to worsen in future climates [7].

Understanding how hydro-climatological shifts impact the potential water needs of crops is therefore important for assessing livelihood risks in Africa. Gaining this understanding depends on a full assessment of changes in both water supply (precipitation) and demand (potential evapotranspiration, hereafter ‘ $E_p$ ’). To conduct such an analysis, it is necessary to have reliable data on all key drivers of  $E_p$ , which include temperature, windspeed, humidity, and

 Content from this work may be used under the terms of the [Creative Commons Attribution 3.0 licence](http://creativecommons.org/licenses/by/3.0/). Any further distribution of this work must maintain attribution to the author(s) and the title of the work, journal citation and DOI.

radiation [8]. Failing to account for all these variables may lead to misleading conclusions about water cycle changes [9], thereby clouding understanding of global change impacts. For example,  $E_p$  calculated from pan evaporation measurements (which integrates all four variables) in Australia and New Zealand showed 30-year trends that are opposite to those calculated from the more commonly used temperature and precipitation-based Thornthwaite model [9]. At a global scale, using the latter model to calculate the Palmer Drought Severity Index suggests more severe drought trends since the 1950s than a variant of the index that incorporates all four  $E_p$  drivers [8]. These differing conclusions are caused by the Thornthwaite model's inability to factor in declines in windspeed, radiation, and vapor pressure deficit, which offset the upwards pressure that increasing temperature exerts on  $E_p$  [9]. This discrepancy is illustrated by recent trends in southwestern South Africa, where declining wind speeds reduced annual evaporative demand between 1974 and 2005, despite a nearly 1 °C rise in temperature, suggesting a reduction in plant water stress [10] during this region's winter rainfall period when its primary crop (wheat) is grown.

Despite the importance of conducting full, physically based assessments of  $E_p$ , undertaking such analyses at large scales is difficult because spatially comprehensive, long-term data on windspeed, humidity, and radiation are either unavailable or unreliable in many parts of Africa. In this study, we use a new bias-corrected meteorological forcing dataset to calculate fully parameterized estimates of  $E_p$ . We identify trends in both precipitation and  $E_p$  to evaluate how water supply, demand, and availability is changing, and examine the factors responsible for the identified changes. To better understand the implications of these findings for food security, we investigate these dynamics within the context of the typical growing season and current production regions for maize, one of Africa's most widely grown and consumed crops [11, 12].

## 2. Datasets and methods

### 2.1. A bias-corrected, gridded meteorological dataset

The forcing data used in this study (excluding radiation) were drawn from the Princeton University global meteorological forcing dataset (PGF; [13]), which consists of three-hourly, 1.0° resolution fields of near-surface meteorology for global land areas for 1948-2012. The PGF merges data the NCEP-NCAR reanalysis (National Center for Environmental Prediction and National Center for Atmospheric Research; [14]) with data from the Global Precipitation Climatology Project, [15], TRMM Multi-Satellite Precipitation Analysis [16], and the Climatic Research Unit's observation-based precipitation and temperature [17]. PGF precipitation, temperature, pressure, specific humidity, and windspeed data were downscaled to 0.25° resolution using bilinear interpolation (with corrections to temperature and humidity based on elevation; see [13]).

The datasets contributing to the downscaled PGF gridded product contain spurious trends and biases due to changes in instruments, observing practices, station environment, satellite sensors, and observation network configuration and density [18]. Following [19], spurious trends were detected using the Pettitt Test [20] for step changes, then removed using the cumulative distribution matching technique. Daily air temperature, wind speed, precipitation, and specific humidity were then bias-corrected by merging quality controlled and gap-filled global summary of day (GSOD) station data [21] (pressure was not corrected due to insufficient observations). The bias-correction consisted of spatially interpolating the differences between GSOD observations and the corresponding value in the co-located grid cell using state-space estimation. This created a spatially explicit correction field for each variable at each time step, which was then added to the original downscaled PGF gridded values to create the bias-corrected data. Online appendix S1, available at [stacks.iop.org/erl/9/075005/mmedia](http://stacks.iop.org/erl/9/075005/mmedia), describes this process in further detail.

We obtained updated short- and longwave radiation datasets from the University of Maryland [22, 23], at 0.5° and 1.0° resolution, respectively, and downscaled these to 0.25° using bilinear interpolation, correcting longwave radiation for elevation [13].

### 2.2. Calculating changes in water supply and demand, and its drivers

The balance between water available for plants (provided by precipitation, P) and atmospheric water demand ( $E_p$ ) is expressed by the ratio  $P/E_p$  (also known as the aridity index [24]), thus trends in either the numerator or denominator will alter this balance. As  $P/E_p$  falls below 1, plant water use (actual evapotranspiration) becomes increasingly limited by supply, whereas demand has a greater influence on use for ratios greater than 1 [9]. To estimate demand, we used the variant of the Penman equation [25] provided by [26] to calculate  $E_p$  (in mm d<sup>-1</sup>). We chose this model over the FAO-56 variant [27] because it clearly separates the radiative and aerodynamic terms. This feature has facilitated the derivation of equations for identifying the main factors driving changes in demand [28], which was a goal of our analysis (see final paragraph in this section). The model is:

$$E_p = \frac{\Delta}{\Delta + \gamma} R_n + \frac{\gamma}{\Delta + \gamma} \frac{6.43(1 + 0.536u_2)D}{\lambda} \quad (1)$$

Where  $\Delta$  (KPa K<sup>-1</sup>) is the slope of saturation vapor pressure curve in relation to temperature,  $\gamma$  is the psychrometric constant (KPa K<sup>-1</sup>),  $R_n$  is net radiation (mm d<sup>-1</sup>), calculated using a fixed albedo (0.23, per [27]), D is the vapor pressure deficit (KPa),  $u_2$  is windspeed (m s<sup>-1</sup>) at 2 m height, and  $\lambda$  is the latent heat of vaporization (MJ mm<sup>-1</sup>). The constants 6.43 and 0.536 are respectively in units of MJ d<sup>-1</sup> KPa<sup>-1</sup> and s m<sup>-1</sup>. Because we were interested in assessing the impacts of changing supply and demand on water availability for maize, we confined  $E_p$  calculations to the days in each year during which maize is grown, using gridded crop

calendar data from [29] to define the start and end of the season. In areas where two maize-growing seasons were identified, we used the dates corresponding to the longest of the two seasons. Since maize sensitivity to water stress varies throughout its growth cycle, we also divided each growing season into three equal sub-intervals, roughly corresponding to maize (1) planting and vegetative development, (2) flowering and grain-filling, and (3) ripening through harvest [30].

We calculated the mean daily  $P$ ,  $E_p$ , and  $P/E_p$  for each full growing season in the time series (which resulted in 31 seasons total, because southern hemisphere maize seasons span calendar years—to be consistent, we excluded 2010 from the northern hemisphere analysis), as well as for the first and second sub-intervals (i.e. the first and second thirds) of the season (the two periods when maize is most sensitive to moisture stress [30]), for each  $0.25^\circ$  grid cell. We used the Kendall–Theil robust line [31], a non-parametric regression used widely in climatological analyses because it has low sensitivity to outliers (e.g., [17, 32]), to calculate the trend slope across the 31 growing seasons and each of the 31 sub-seasons.

To further improve the relevance of our analysis to maize production impacts, we examined changes in supply, demand, and aridity index only in areas where maize is grown (defined using maps of crop area from [33]), and to boost confidence in the detected trends we only examined those cells where the forcing data received a minimum level of bias correction by station data (determined by a weighting term described in appendix S1). We therefore confined our analyses to those maize-producing cells (1) within countries where at least 20% of cells support maize production (to select the most important maize-growing regions), and (2) 20% of those cells received the minimal level of bias correction (appendix S1 provides further details of the area selection criteria). We then calculated, from these selected cells, the average country-level trends for the three variables ( $P$ ,  $E_p$ , and  $P/E_p$ ), as well as the statistical distributions of cell-level trends, segregated by region (East Africa, Southern Africa, and West Africa).

To assess the sensitivity of results to the specified growing season and the analyzed maize-growing area, we performed two sets of sensitivity tests. In the first set, to test how area impacted results, we changed the bias correction weighting threshold from 0.25 (the value used for the main analysis, see appendix S1) to 0.05 and 0.5. In the second set, we altered the number of days included in the full growing season, adjusting planting and harvesting dates by equal numbers of days to either lengthen or shorten the growing season by 20%. We then re-ran the full growing season  $P$  and  $E_p$  trend analyses for these four sets of data, and examined how much their country-level  $P$  and  $E_p$  trend results differed from those of the main analysis.

The trend analyses indicated whether changes in water availability within the selected maize-growing areas were being driven by changes in supply, demand, or both. To understand the factors driving demand changes, we used the partial derivatives developed by [34] to attribute trends in  $E_p$  to changes in temperature, net radiation, windspeed, and actual vapor pressure (see appendix S1 for methods).

### 3. Results

#### 3.1. Selected regions

The two area selection criteria (see 2.2.) identified twenty-one countries (five in East Africa, seven in Southern Africa, and nine in West Africa) containing 3,346 grid cells (figure 1), which comprise 34% of all maize-growing cells in Africa, and an average of 63% (range = 20–100%) of each countries' maize-growing cells. The average growing season aridity index ( $P/E_p$ ) in each cell (figure 1) reveals substantial variability in supply-demand balance throughout the maize-growing region, ranging from areas where supply is the main limiting factor (e.g.,  $P/E_p$  in Kenya = 0.52) to those where demand is the primary constraint on maize water use ( $P/E_p$  in Guinea-Bissau = 3.22). Substantial within-country variability in  $P/E_p$  is also evident, e.g. in Ethiopia and Mozambique (figure 1).

#### 3.2. Spatial trends in supply and demand

The 31-year trends in growing season  $P$ ,  $E_p$ , and  $P/E_p$  over the selected areas show substantial spatial variation (figure 2), particularly precipitation trends. The Sahelian zone (Ethiopia and the more northern West African countries) had increasing rainfall, while immediately to the south—in Kenya, Rwanda, and Burundi, and along West Africa's Gulf of Guinea—supply trends were flat or declining. Southern African countries had patchy rainfall change patterns, with small areas of increases (southern Zimbabwe) and decreases (central Malawi) flanked by somewhat larger areas of little or no change.  $E_p$  trends were more spatially coherent, and the most prominent patterns were the large  $E_p$  declines ( $0.02$ – $0.04$   $\text{mm d}^{-1}\text{yr}^{-1}$ ) over South Africa and the West African Sahelian countries, with lower magnitude declines ( $0.01$ – $0.02$   $\text{mm d}^{-1}\text{yr}^{-1}$ ) over Zimbabwe and Ethiopia. The northern parts of southern Africa, East Africa (excluding Ethiopia), and the Gulf of Guinea generally had no change in demand.

These supply and demand changes underlie the trends in  $P/E_p$  (figure 2, bottom). In South Africa, declining  $E_p$  was primarily responsible for increasing the  $P/E_p$  ratio over most of the country, thereby making it less arid. Southern Zimbabwe showed a similar pattern, but increasing precipitation was more important. Malawi's  $P/E_p$  fell due to declining rainfall, while the pattern of aridity changes in East Africa was more mixed and also driven by rainfall trends—Tanzania and Burundi generally became more arid, Rwanda became wetter, and Kenya remained mostly unchanged, with smaller patches of increasing aridity in the north, center (coinciding with the highlands), and southwest, and a small island of increasing wetness in the west. Aridity declines in the Sahelian belt were due to a combination of increasing supply and (to a lesser extent) reduced demand, while the drying in the Ivory Coast and western Cameroon was primarily due to reduced  $P$ .

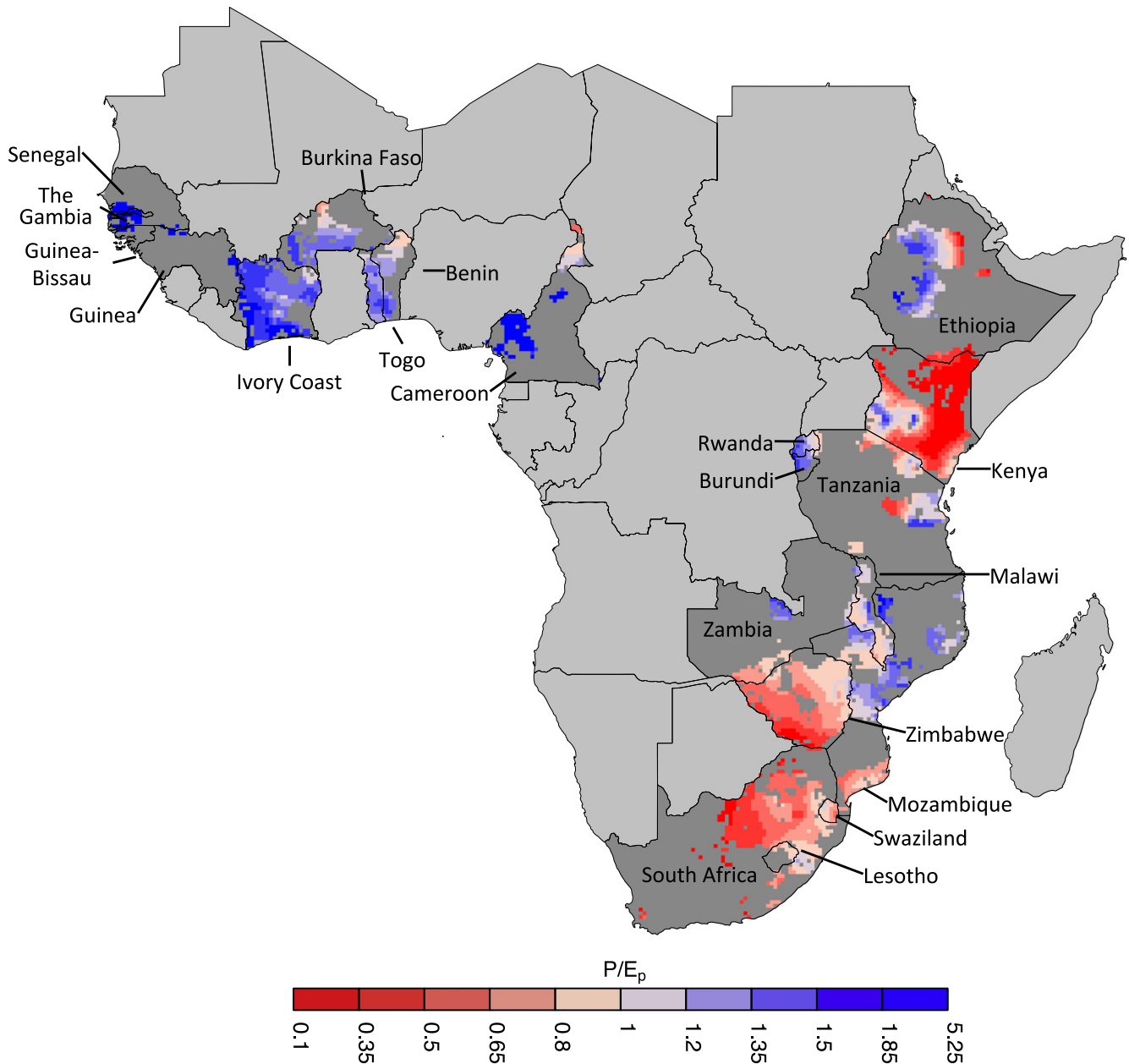


**Figure 1.** The countries and maize-growing grid cells included in the trend analysis. Countries having at least 20% of 0.25° grid cells containing maize production, and ≥ 20% of these cells having minimum bias-correction applied to their forcing data, were selected. Selected countries are shaded dark grey, and the selected maize-growing cells are colored according to their average growing season P/E<sub>p</sub>. Redder colors indicate increasing supply limitation (P/E<sub>p</sub> < 1) while bluer colors indicate increasing demand limitation (P/E<sub>p</sub> > 1).

### 3.3. Country-level trends in supply and demand

We averaged cell-level trends to estimate country-level water availability changes and their causes during the full, early, and middle growing seasons for maize (figure 3, and table 1 in appendix S2). We assessed trends in supply, demand, and availability (figure 3, left column), as well as the percent change implied by these trends relative to their time series mean values (figure 3, center column, for P and E<sub>p</sub>; right column for P/E<sub>p</sub>—table 1 in appendix S2 provides P/E<sub>p</sub> trend coefficients). Estimating trend impacts in this way (per equation (1), appendix S2) offers greater insight into the impacts of P and E<sub>p</sub> changes on water availability, as it

accounts for imbalances in supply and demand (as reflected by P/E<sub>p</sub>; figure 3, right column).

In more than half of all countries and in all assessed seasons, supply increased while demand declined, as illustrated by the countries falling within the lower right quadrants of figure 3's left column (some are not illustrated because of large positive precipitation trends; their values are given in table 1, appendix S2). The average absolute trend in P was 2.2-3.6 times larger than that of E<sub>p</sub>, depending on the seasonal period analyzed (reflected in the scaling of axes in figure 3), indicating that supply changes were larger during this time period. The most pronounced examples of this were The Gambia and Senegal, where P



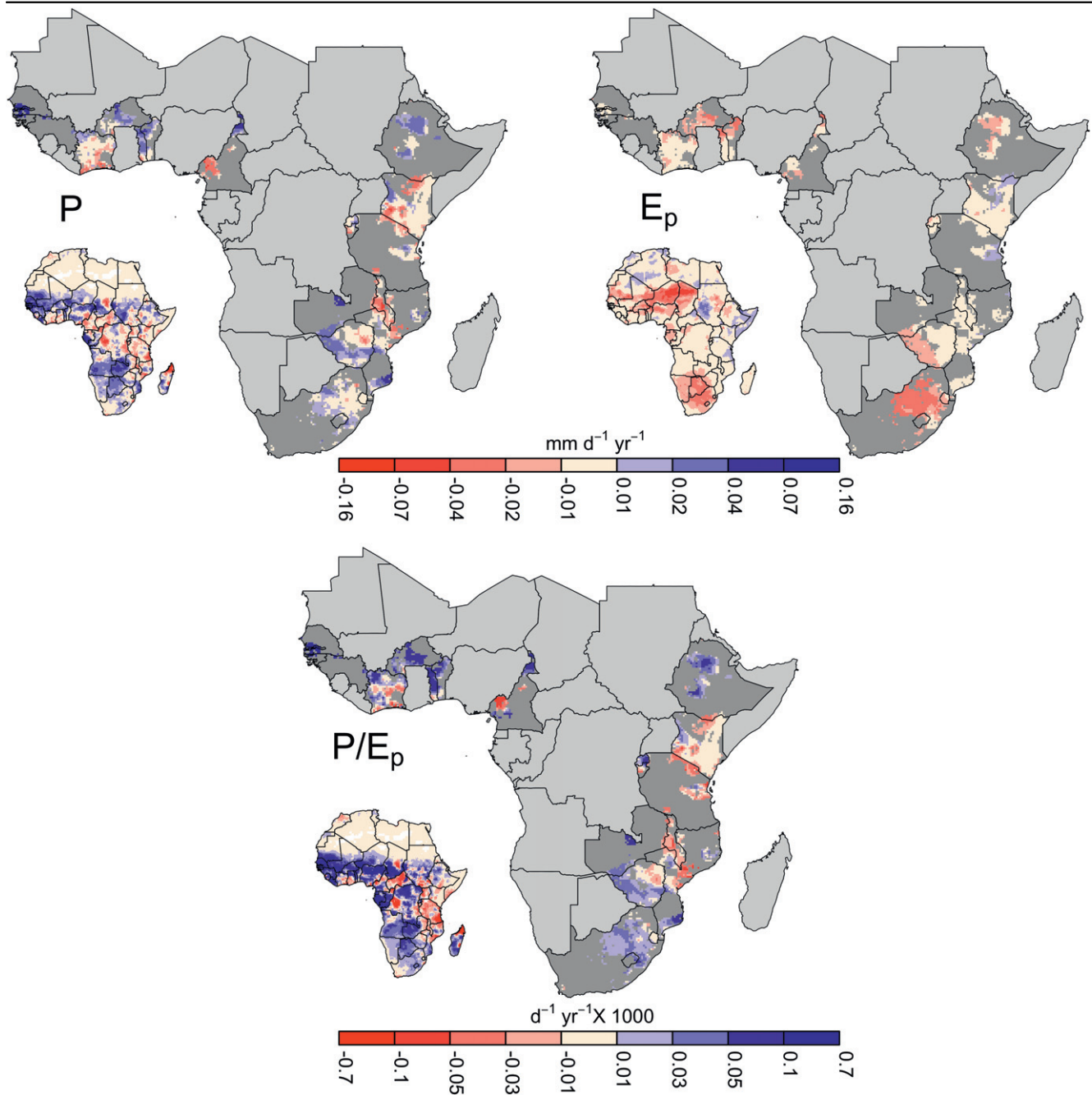


**Figure 2.** Trends (1979–2010) in precipitation (P, top left),  $E_p$  (top right), and  $P/E_p$  (bottom) in the maize-growing areas and countries (dark grey) selected for analysis (main maps). Inset maps show the trends for each variable for every  $0.25^\circ$  grid cell in Africa. Values for P and  $E_p$  trends are given in  $\text{mm d}^{-1}\text{yr}^{-1}$ , whereas (the unitless)  $P/E_p$  trends ( $\text{d}^{-1}\text{yr}^{-1}$ ) are multiplied by 1000 for legibility.

trends imply 27 and 26% growing season supply increases during the 31-year period, while  $E_p$  declined by less than 3%. These changes translate to water availability ( $P/E_p$ ) increases of 30 and 28% (table 1, appendix S2). South Africa and Cameroon represent the opposite extreme, in that demand reductions contributed more than supply gains to increased water availability. These two countries also represent the extremes of water and energy limitation. South Africa, with an aridity index of 0.61, had only a slight P trend ( $<0.008 \text{ mm d}^{-1}\text{yr}^{-1}$ ), but because mean P is low there this translated into an implied 11% supply gain, making its

impact in reducing aridity larger than the trend magnitude would suggest, albeit still less important than the 16% reduction in  $E_p$ . Cameroon’s rainfall is twice that of  $E_p$ , so a small trend ( $-0.008 \text{ mm d}^{-1}\text{yr}^{-1}$ ) resulted in a 7% decline in demand, which was most of the 8% increase in water availability implied by the  $P/E_p$  trend.

In the middle, three countries—Lesotho, Benin, and Bukina Faso—had large increases in growing season water availability (26%, 17%, and 18%) that were equally partitioned between supply increases (+10–12%) and demand reductions (–10–12%). In a few cases, demand reductions

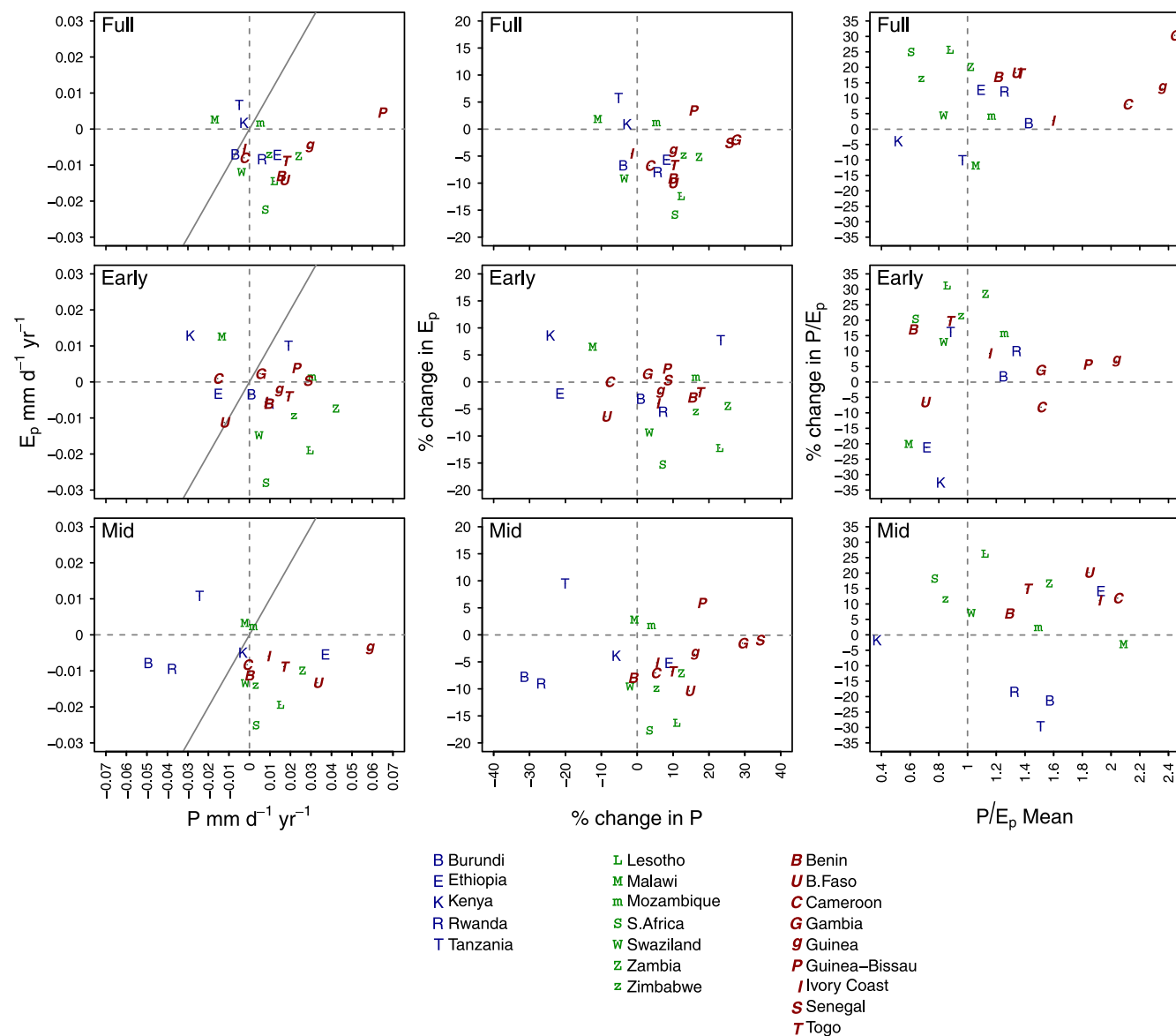


**Figure 3.** Country-averaged trends in  $P$ ,  $E_p$ , and  $P/E_p$ , for the full (top row), early (center row), and middle (bottom row) growing seasons. The left column plots trends in  $P$  versus  $E_p$  in  $\text{mm d}^{-1}\text{yr}^{-1}$ , with a solid line indicating the point where trends in  $P$  and  $E_p$  offset one another when  $P/E_p = 1$ . The center column expresses the percent change in  $P$  and  $E_p$  implied by their trends, relative to the 1979–2010 seasonal average value for each variable. The right column plots the time series mean  $P/E_p$  versus the percent change implied by its trend; the vertical dashed line in these panels indicates the point of transition between energy (right of the line) and water-limited (left of the line) systems.

offset decreased supply, leading to small increases in  $P/E_p$  (e.g., Swaziland, +4%; Ivory Coast, +3%).

Only three countries experienced increasing aridity during the full growing season. Malawi’s  $P/E_p$  ratio declined by 12%, driven primarily by reduced rainfall, while Tanzania’s ratio fell 10% due to a supply reduction and demand increase of equal magnitudes. Kenya had a very small (4%) reduction in water availability, due mostly to reduced rainfall.

These full season patterns are representative of the changes that occurred within sub-seasons, with notable exceptions in several (mostly) East African countries where availability changed substantially between the early and mid-seasons (figure 3 and table 1, appendix S2). Rwanda’s  $P/E_p$  ratio increased 10% during the early season, but

declined 28% during the middle season, driven by a large reduction in rainfall, and Burundi showed nearly the same sub-seasonal differences. Kenya showed the opposite: a large increase in aridity during the early growing season ( $\Delta \% P/E_p = -33\%$ ), caused by a 24% decline in  $P$  and a 9% demand increase, but almost no change during the mid-season. Ethiopia presented a similar case, having a 21% early season decline in  $P/E_p$  followed by a mid-season gain of 14%. Unlike the previous East African examples, Ethiopia switches from water to energy limitation between the two sub-seasons ( $P/E_p$  early = 0.72; mid = 1.93). Malawi, a southern Africa country, had nearly the same pattern of limitation and change. Three West African countries (Benin, Togo, Burkina Faso) also had intra-

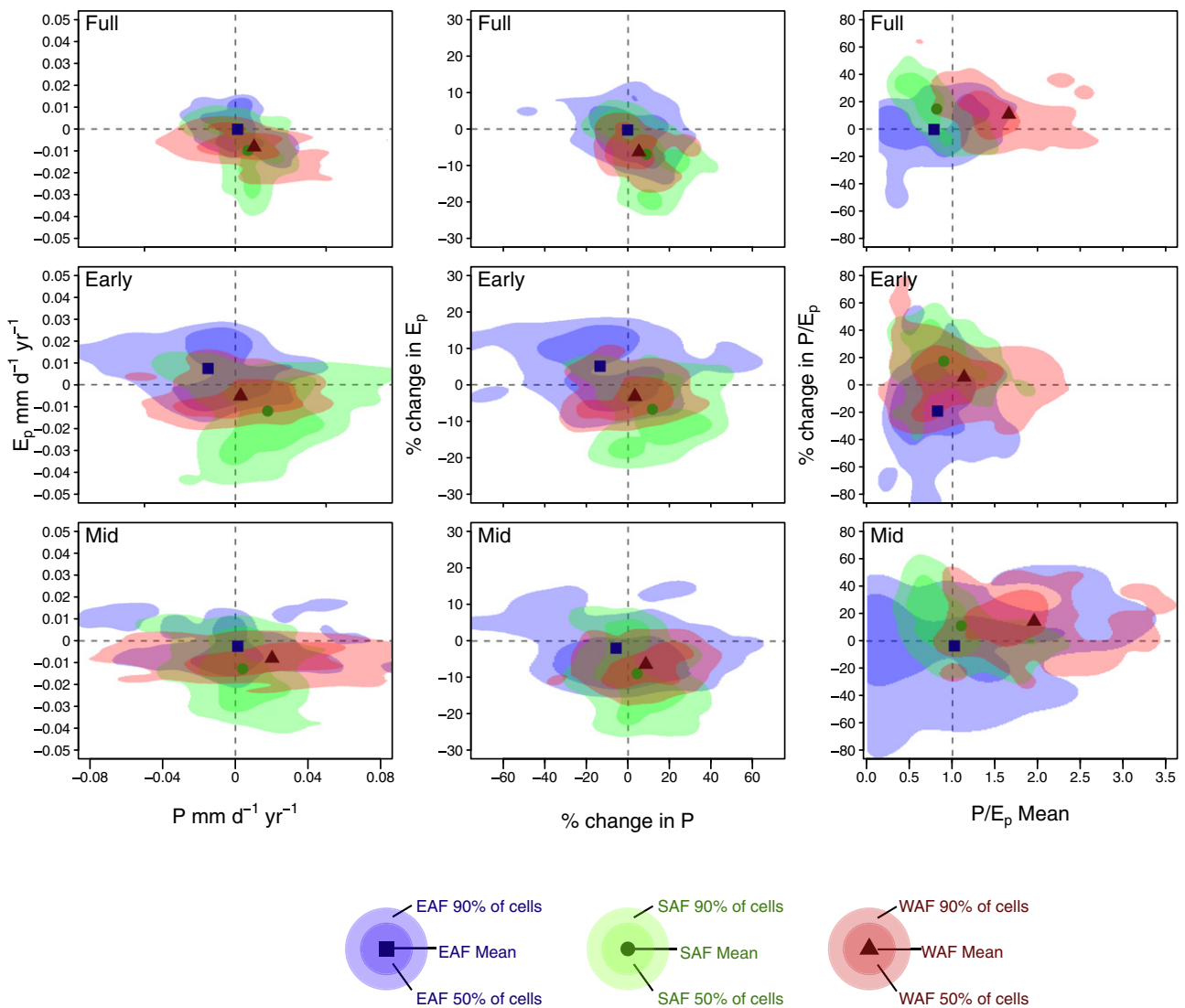


**Figure 4.** The distributions of cell level trends in P, E<sub>p</sub>, and P/E<sub>p</sub>, for the full (top row), early (center row), and middle (bottom row) growing seasons. The left column plots trends in P versus E<sub>p</sub>, in mm d<sup>-1</sup> yr<sup>-1</sup>, segregated by color into the three primary regions (East Africa, Southern Africa, West Africa), where the lightest shade indicates the contour within which 90% of all regional trend values are contained, the darker shade shows the 50% contour, and the point symbol gives the regional mean value. The center column shows the percent change in P and E<sub>p</sub> implied by their trends, relative to the 1979–2010 seasonal average value for each variable. The right column plots the time series mean P/E<sub>p</sub> versus the percent change implied by the trend in P/E<sub>p</sub>; the vertical dashed line indicates the point of transition between energy (right of the line) and water-limited (left of the line) systems.

seasonal changes in supply-demand balance, but water availability increased in these countries in both seasons, except for Burkina Faso where early season P/E<sub>p</sub> declined (−7%).

Examining the within-region statistical distributions of the trend metrics from individual maize-growing cells (figure 4) gives a fuller sense of the variability in the patterns of change in supply, demand, and availability. Southern Africa’s maize-growing areas mostly experienced water limitation during the full season, but there was a tendency towards increasing water limitation, as evidenced by the fact that most cells fall below zero and above one on figure 4’s x and y axes, respectively. The region’s average P/E<sub>p</sub> was 0.82, and regional water availability increased by 15% (dark green circle in figure 4 upper right). West African maize-growing areas were also fairly consistent in being energy-

limited (mean P/E<sub>p</sub> = 1.7) and having increased water availability (mean change in P/E<sub>p</sub> = 11%). East Africa was the most variable: although the region was on average water-limited (P/E<sub>p</sub> = 0.78), a large share of its maize-growing area was energy-limited, and the water availability changes were evenly split between declines and increases such that the mean percent change was 0.

Regional variability was substantially greater at the sub-seasonal level. In the early season, West Africa was more equally divided between areas of increased and decreased water availability, with a low mean percent change (+5%), and the region had a larger share of areas experiencing supply limitations (mean P/E<sub>p</sub> = 1.1). During the mid-season, the regional variability in E<sub>p</sub> trends narrowed, while P trend variability broadened, primarily in the direction of increasing supply. This resulted in water availability gains of 14%



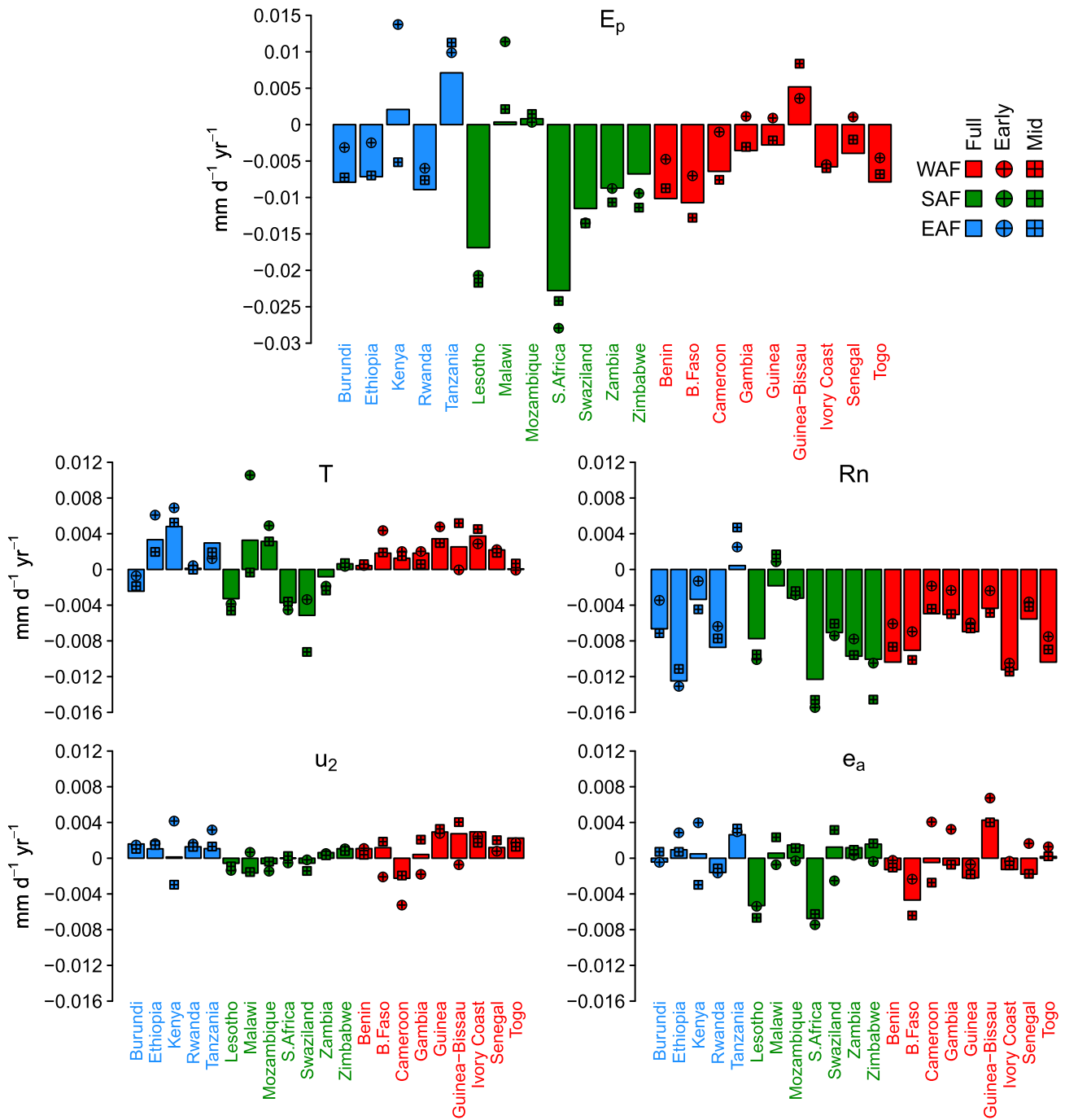


**Figure 5.** Mean trends in  $E_p$  for each country’s maize-growing region (top), and the attribution of those trends to changes in temperature ( $T$ ), net radiation ( $R_n$ ), windspeed ( $u_2$ ), and actual vapor pressure ( $e_a$ ). Bars indicate the trends and attributions for the full growing season, while crossed circles and squares respectively represent the same values for the early and mid growing season. Country values are color-coded by region.

accompanied by a pronounced shift into a demand-limited state (mean  $P/E_p = 2$ ). In the early season, East African maize-growing areas had a broad distribution of  $P$  and  $E_p$  trends, but the region had an average availability decrease of 19%. East Africa’s mid-season water availability distributions exhibited the largest variation of all regions and seasons, spread equally around decreases and increases (mean % change in  $P/E_p = -4\%$ ), and straddling the domains of water and energy limitation (mean  $P/E_p = 1.02$ )

**3.4. Sensitivity of trends to season length and selection criteria**

The country-level supply and demand trends were relatively insensitive to the size of the maize-growing region, but were substantially impacted by growing season length (see figure 3, appendix S2). Lowering the bias correction threshold to 0.05 altered  $P$  and  $E_p$  trend estimates by just 4% relative to our main findings. Increasing the threshold to 0.5 resulted in a much smaller area being considered (only seven countries

**Table 1.** Mean contribution (in mm d<sup>-1</sup>yr<sup>-1</sup>) of each of the four E<sub>p</sub> trend drivers (temperature, T; net radiation, R<sub>n</sub>; wind speed, u<sub>2</sub>; actual vapor pressure; e<sub>a</sub>) at the regional and sub-continental scales, as well as the mean E<sub>p</sub> trends.

	T	R <sub>n</sub>	U <sub>2</sub>	e <sub>a</sub>	E <sub>p</sub>
E. Africa	0.0038	-0.0052	0.0006	0.0009	0.0001
Sthn Africa	-0.0003	-0.0086	0.0001	-0.0014	-0.0102
W. Africa	0.0023	-0.0093	0.0015	-0.0016	-0.0071
Africa <sup>a</sup>	0.0016	-0.0077	0.0006	-0.0007	-0.0062

<sup>a</sup> Sub-Saharan Africa

remained), but the mean P and E<sub>p</sub> trend differences (relative to the main results) were just 13% and 9%, respectively. A longer growing season resulted in 28% and 18% differences for P and E<sub>p</sub> trends, respectively, while shortening the season caused 20% differences for trends in both variables. Several countries' trends changed sign, particularly those with trend magnitudes close to zero.

### 3.5. Drivers of demand trends

To better understand the more complex factors determining demand changes, we used the attribution analysis to decompose E<sub>p</sub> trends into their four driving components. Figure 5 confirms that E<sub>p</sub> trends were generally of the same direction and similar magnitude when calculated for the full, early, and mid-growing season (note: these E<sub>p</sub> trends were calculated by summing the four attribution components per [34], which produces slightly different values than the Kendall–Theil trend calculated over the E<sub>p</sub> time series; comparisons indicate the differences are insignificant and thus not shown here). Several countries' demand trends switched sign between the early and mid-growing seasons, but these were generally of negligible magnitude—the most pronounced of these was Kenya, where the early season E<sub>p</sub> trend was 0.014 mm d<sup>-1</sup>yr<sup>-1</sup> compared to -0.005 mm d<sup>-1</sup>yr<sup>-1</sup> in the mid season.

The trend attribution analysis revealed the variables driving changes in demand (figure 5, lower panels). Temperature exerted small to modest upwards pressure on E<sub>p</sub> in 12 countries, with the largest effects in East Africa (figure 3, T panel), where it contributed 0.003 (Ethiopia) to 0.005 mm d<sup>-1</sup>yr<sup>-1</sup> to demand in Ethiopia, Kenya, and Tanzania during the full growing season. Temperature also added to demand in all 7 West African countries, but its impact there was smaller (0.001–0.004 mm d<sup>-1</sup>yr<sup>-1</sup>). In southern Africa temperature's impact was mixed, ranging from small positive contributions (0.003 mm d<sup>-1</sup>yr<sup>-1</sup>) in Malawi and Mozambique, to demand reductions of slightly larger magnitude in South Africa, Swaziland, and Lesotho (0.003–0.005 mm d<sup>-1</sup>yr<sup>-1</sup>). Net radiation's contribution to E<sub>p</sub> trends was largest and most uniform, putting downwards pressure on E<sub>p</sub> in all countries but Tanzania, with the greatest impacts in Ethiopia and South Africa, where radiation-driven reductions were ≥0.012 mm d<sup>-1</sup>yr<sup>-1</sup>, while eight more countries across the 3 regions had reductions ≥0.008 mm d<sup>-1</sup>yr<sup>-1</sup>. Actual vapor pressure (hereafter 'vapor pressure') had lower and more mixed impacts on E<sub>p</sub> trends,

followed by wind speed, which was even less significant. The only notable effects of vapor pressure were in South Africa, Lesotho, and Burkina Faso, where it put downwards pressure on E<sub>p</sub> of 0.005–0.007 mm d<sup>-1</sup>yr<sup>-1</sup>, and in Guinea–Bissau, where it added 0.004 mm d<sup>-1</sup>yr<sup>-1</sup>. The largest impact of windspeed was the very slight upwards pressure it exerted on E<sub>p</sub> in three West Africa countries, Guinea, Guinea–Bissau, and Ivory Coast (0.003 mm d<sup>-1</sup>yr<sup>-1</sup>), followed by a small downwards impact in Cameroon (-0.002 mm d<sup>-1</sup>yr<sup>-1</sup>).

Although neither vapor pressure nor windspeed had an appreciable impact on full season E<sub>p</sub> trends in East Africa, there were modest and divergent sub-seasonal impacts for these two variables in Kenya, where both added upwards pressure of (0.004 mm d<sup>-1</sup>yr<sup>-1</sup>) during the early season, and were thereby responsible for most of this sub-season's positive E<sub>p</sub> trend. In the mid-season the impacts were reversed, as both drivers contributed downwards pressure (-0.003 mm d<sup>-1</sup>yr<sup>-1</sup>) causing much of the E<sub>p</sub> decline.

Averaging the attributions by region provides a ranking of the relative importance of each variable in driving large-scale water demand trends (table 1). Across East Africa, net radiation had the greatest impact, followed by temperature, and then distantly by vapor pressure and windspeed, with all effects largely canceling each other out. In southern Africa net radiation and vapor pressure dominated, while temperature and windspeed had negligible effects. Net radiation was the most influential demand driver in West Africa, followed by temperature, vapor pressure, and wind speed. Across Sub-Saharan Africa, net radiation was most important, followed by temperature, then distantly by vapor pressure and windspeed.

## 4. Discussion

Our results indicate generally increasing water availability for maize during its primary growing season, and within much of its growing region, in sub-Saharan Africa. Most of this change was due to increases in supply, particularly in the Sahelian zone (West Africa through Ethiopia), which was recovering from multi-decadal droughts [35] during the period of this study. In a few areas, particularly the southern Africa countries of South Africa and Lesotho, reduced atmospheric demand played an equally important, or dominant, role. A few countries centered around the East African country of Tanzania experienced water availability declines due to a combination of reduced rainfall and demand increases, including the neighboring southern African country of Malawi and the southwestern parts of Kenya. But the increases elsewhere in East Africa, particularly Ethiopia and Rwanda, completely neutralized these declines at the regional scale, such that East Africa experienced no net change in water availability during the full maize-growing season.

The regional assessment of trends reveals that supply changes were much more variable than shifts in demand, particularly in East and West Africa, and this was particularly true at the intra-seasonal scale. Ethiopia, Rwanda, Tanzania, and Burkina Faso's early and mid-season supply trends are

examples (figure 3) that suggest increased intra-annual rainfall variability and changes in seasonality. The variability in change patterns within East Africa, particularly for rainfall, has been reported from other studies [17], and may reflect the interplay between the more complex seasonality in East Africa (which has bimodal rainfall) and the El Niño Southern Oscillation and Indian Ocean dipole [36].

In contrast to supply change patterns, demand shifts tended to be more spatially coherent, had less intra-seasonal variation in magnitude (e.g., South Africa), and rarely changed sign (Kenya being an exception). Declining net radiation reduced atmospheric water demand almost uniformly in all countries, and in general counter-acted, and often over-rode, the upwards pressure that temperature placed on demand in most East and West African countries. Temperature's influence was more mixed in southern Africa, pushing downwards on  $E_p$  in this region's southern countries, but upwards in the north. Vapor pressure's impacts were more mixed and mostly negligible, except in South Africa and Lesotho, where it combined with temperature and net radiation to drive the largest demand reductions measured in this analysis. Overall, these results are similar to findings from Australia, where  $E_p$  fell between 1981–2006 due to net radiation and windspeed declines and increasing vapor pressure [34]. However, that study showed temperature to be the largest impactor of demand (exerting upwards pressure), while our results suggest net radiation was more significant. We also found that windspeed had a negligible impact, whereas [34] found falling windspeed to be the biggest factor behind Australian  $E_p$  declines, as have studies of pan evaporation trends elsewhere ([10, 37] and citations therein). Our results suggest that stiling in sub-Saharan Africa has not occurred, which either reflects a real atmospheric feature during the maize-growing season (implying that wind reductions largely occur in the dry seasons), or residual biases in our forcing data. Within the context of this study, there are insufficient station data at the scales of our analysis to rule out either possibility (a supplementary analysis of trends in co-located forcing data and station observations in appendix S2 provides further support for this statement).

These findings have important implications for the production of maize and concurrently grown crops. The most prominent result is the strong demand-driven water availability increase over South Africa, which should have provided substantial gains for Africa's (and the World's 9th) largest maize producer [12, 38]. Although South Africa is strongly water-limited ( $P/E_p = 0.61$ ), suggesting that South African maize would primarily benefit from increased supply rather than reduced demand [1, 9], a large portion of South Africa's maize is grown between the 400–500 mm isohyets [39] where irrigation is widely used, thus the strong  $E_p$  declines should have reduced irrigation demands. On the other hand, reduced evaporative demand could have exacerbated maize heat stress by lowering transpiration, thereby increasing leaf temperatures [10, 40]. However, temperatures also fell (figure 3 and appendix S2), and there was no observed increase in the frequency of extreme heat days between 1961–2000 [17], which were not analyzed here but

can have large negative impacts on yields [41]. The question is why South Africa (and its near neighbors) cooled over this period, when nearly every other country experienced at least some warming during the growing season? A large increase in irrigated cropland since 1970 (in the same area showing temperature declines) may have played a role [42], and may also have contributed to the vapor pressure increases. Although this suggestion is speculative, these effects have been linked to increases in irrigated farmland in the US Great Plains [43].

Elsewhere the picture for maize production is more mixed, and perhaps less positive. Although the Sahelian region experienced rainfall increases, many of these countries had substantial, intra-seasonal differences in availability trends, including switches from water to energy limited regimes. If these translated to increasing rainfall variability, this is likely to have negatively impacted livelihoods in these subsistence farming-dependent countries [1, 7]. Additionally, since this region is primarily energy-limited during the growing season, a larger portion of the increased rainfall is likely to have gone to runoff rather than maize transpiration [9]. In parts of East Africa, where availability decreased the most and sub-seasonal changes were greatest, negative impacts on maize crops were likely largest, particularly since some of the largest supply declines occurred during the highly sensitive mid-season [5, 30], and coincided with increases in extreme heat days [17], which further exacerbate maize water stress [41].

Some caution must be attached to our findings, since they are based on a reanalysis dataset that may contain biases. Although we made substantial efforts to remove these biases, identifying residual errors and how much they influence our results is difficult, as our windspeed-related findings illustrate. Assumptions made in calculating  $E_p$  may also play a role, such as the use of a fixed albedo term and its potential impact on net radiation estimates [34]. However, given that African cropland area increased [44] while forest cover declined [45, 46] during the period of our analysis, and land use in South Africa has remained fairly stable since the 1960s [47], it seems unlikely that albedo has declined below this fixed value (which would have caused us to overestimate net radiation declines). The exception to this lies in the regreening Sahelian zone [35], although the value we used (0.23) may be too low for this region in any case [48], in which case we overestimated net radiation. Nevertheless, future work should investigate how albedo has changed during the same time period, and how this has affected demand trends.

We also relied on two radiation datasets that we did not bias-correct. Although these data are best in class and were validated against observations [22, 23], they may have biases that affect our net radiation results. Arguing against this is the observed global dimming between 1960–1990, which continued into the 2000s in developing regions (Asia) as a result of increasing aerosol pollution [49, 50]. There are no studies to confirm this trend over Africa [49], but southern African sulfur dioxide concentrations increased through 2000 [50], which could contribute to dimming and thereby explain our estimated net radiation declines.

A final caveat is the sensitivity of trend results to the growing season interval, but given the sub-seasonal variability seen in several areas, combined with this region's pronounced rainfall seasonality (to which maize-growing seasons are aligned) and reported hydro-climatological shifts [17], this sensitivity is not surprising. A more important concern is how closely the planting date estimates we used [29] align with actual African maize production seasons.

Despite these potential shortcomings, our results should provide valuable insight into where and why water cycle dynamics have changed in much of sub-Saharan Africa's maize-producing regions, and how these shifts might have impacted water availability for this crucial staple crop. As such, these findings may help inform regional food security and climate change impacts assessments.

## Acknowledgments

We thank the United States Army Corps of Engineers Institute for Water Resources (IPA 130019), the NASA Measures Program (NNX14AB36A), and Princeton Environmental Institute Grand Challenges Program for funding that supported this research.

## References

- [1] Rockström J 2000 Water resources management in smallholder farms in eastern and southern Africa: an overview *Phys. Chem. Earth B: Hydrol. Oceans Atmos.* **25** 275–83
- [2] Burney J A, Naylor R L and Postel S L 2013 The case for distributed irrigation as a development priority in Sub-Saharan Africa *Proc. Natl. Acad. Sci.* **110** 12513–7
- [3] Morris M and Byerlee D 2009 *Awakening Africa's Sleeping Giant Technical Report* (Washington, DC: World Bank)
- [4] D'Odorico P and Bhattachan A 2012 Hydrologic variability in dryland regions: impacts on ecosystem dynamics and food security *Phil. Trans. R. Soc. B* **367** 3145–57
- [5] Barron J, Rockström J, Gichuki F and Hatibu N 2003 Dry spell analysis and maize yields for two semi-arid locations in East Africa *Agric. Forest Meteorol.* **117** 23–37
- [6] Falkenmark M and Rockström J 2008 Building resilience to drought in desertification-prone savannas in Sub-Saharan Africa: the water perspective *Nat. Resour. Forum* **32** 93–102
- [7] Verdin J, Funk C, Senay G and Choularton R 2005 Climate science and famine early warning *Phil. Trans. R. Soc. B* **360** 2155–68
- [8] Sheffield J, Wood E F and Roderick M L 2012 Little change in global drought over the past 60 years *Nature* **491** 435–8
- [9] Hobbins M T, Dai A, Roderick M L and Farquhar G D 2008 Revisiting the parameterization of potential evaporation as a driver of long-term water balance trends *Geophys. Res. Lett.* **35** L12403
- [10] Hoffman M T, Cramer M D, Gillson L and Wallace M 2011 Pan evaporation and wind run decline in the Cape Floristic Region of South Africa (1974–2005): implications for vegetation responses to climate change *Clim. Change* **109** 437–52
- [11] Jones P G and Thornton P K 2003 The potential impacts of climate change on maize production in Africa and Latin America in 2055 *Glob. Environ. Change* **13** 51–59
- [12] FAO 2013 FAO statistical data [www.fao.org/statistics/en](http://www.fao.org/statistics/en)
- [13] Sheffield J, Goteti G and Wood E F 2006 Development of a 50 year high-resolution global dataset of meteorological forcings for land surface modeling *J. Clim.* **19** 3088–111
- [14] Kalnay E *et al* 1996 The NCEP/NCAR 40 year reanalysis project *Bull. Am. Meteorol. Soc.* **77** 437–71
- [15] Adler R F *et al* 2003 The version 2 global precipitation climatology project (GPCP) monthly precipitation analysis (1979–present) *J. Hydrometeorol.* **4** 1147–67
- [16] Huffman G J, Adler R F, Bolvin D T, Gu G, Nelkin E J, Bowman K P, Hong Y, Stocker E F and Wolff D B 2007 The TRMM multisatellite precipitation analysis (TMPA): quasi-global, multiyear, combined-sensor precipitation estimates at fine scales *J. Hydrometeorol.* **8** 38–55
- [17] New M *et al* 2006 Evidence of trends in daily climate extremes over Southern and West Africa *J. Geophys. Res.: Atmos.* **111** D14102
- [18] Klein Tank A M G, Zwiers F W and Zhang X 2009 Guidelines on analysis of extremes in a changing climate in support of informed decisions for adaptation *WCDMP No.72 WMO-TD No. 1500* [http://eca.knmi.nl/documents/WCDMP\\_72\\_TD\\_1500\\_en\\_1.pdf](http://eca.knmi.nl/documents/WCDMP_72_TD_1500_en_1.pdf)
- [19] Chaney N W, Sheffield J, Villarini G and Wood E F 2014 Spatial analysis of trends in climatic extremes with a high resolution gridded daily meteorological data set over Sub-Saharan Africa *J. Clim.* doi:10.1175/JCLI-D-13-00723.1
- [20] Pettitt A N 1979 A non-parametric approach to the change-point problem *J. R. Stat. Soc. Ser. C: Appl. Stat.* **28** 126–35
- [21] Smith A, Neal L and Russ V 2011 The integrated surface database: recent developments and partnerships *Bull. Am. Meteorol. Soc.* **92** 704–8
- [22] Ma Y and Pinker R T 2012 Modeling shortwave radiative fluxes from satellites *J. Geophys. Res.: Atmos.* **117** 1–19
- [23] Nussbaumer E A and Pinker R T 2012 Estimating surface longwave radiative fluxes at global scale *Q. J. R. Meteorol. Soc.* **138** 1083–93
- [24] Zomer R J, Trabucco A, Bossio D A and Verchot L V 2008 Climate change mitigation: a spatial analysis of global land suitability for clean development mechanism afforestation and reforestation *Agric. Ecosyst. Environ.* **126** 67–80
- [25] Penman H L 1948 Natural evaporation from open water, bare soil and grass *Proc. R. Soc. A* **193** 120–45
- [26] Shuttleworth W 1993 *Evaporation Handbook of Hydrology* ed D Maidment (New York: McGraw-Hill)
- [27] Allen R G, Pereira L S, Raes D and Smith M 1998 Crop evapotranspiration-guidelines for computing crop water requirements-FAO irrigation and drainage paper 56 *FAO, Rome* **300** 6541
- [28] Donohue R J, McVicar T R and Roderick M L 2009 Generating Australian potential evaporation data suitable for assessing the dynamics in evaporative demand within a changing climate *Water for a Healthy Country National Research Flagship: CSIRO*
- [29] Sacks W J, Deryng D, Foley J A and Ramankutty N 2010 Crop planting dates: an analysis of global patterns *Glob. Ecol. Biogeogr.* **19** 607–20
- [30] Rojas O, Vrieling A and Rembold F 2011 Assessing drought probability for agricultural areas in Africa with coarse resolution remote sensing imagery *Remote Sens. Environ.* **115** 343–52
- [31] Kendall M G 1975 *Rank Correlation Methods* (London: Charles Griffin)
- [32] Ziegler A D, Sheffield J, Maurer E P, Nijssen B, Wood E F and Lettenmaier D P 2003 Detection of intensification in global and continental-scale hydrological cycles: temporal scale of evaluation *J. Clim.* **16** 535–47
- [33] Monfreda C, Ramankutty N and Foley J A 2008 Farming the planet: 2. geographic distribution of crop areas, yields,



- physiological types, and net primary production in the year 2000 *Glob. Biogeochem. Cycles* **22** GB1022
- [34] Donohue R J, McVicar T R and Roderick M L 2010 Assessing the ability of potential evaporation formulations to capture the dynamics in evaporative demand within a changing climate *J. Hydrol.* **386** 186–97
- [35] Olsson L, Eklundh L and Ardö J 2005 A recent greening of the Sahel-trends, patterns and potential causes *J. Arid Environ.* **63** 556–66
- [36] Black E, Slingo J and Sperber K R 2003 An observational study of the relationship between excessively strong short rains in coastal East Africa and Indian Ocean SST *Mon. Weather Rev.* **131** 74–94
- [37] Roderick M L, Rotstayn L D, Farquhar G D and Hobbins M T 2007 On the attribution of changing pan evaporation *Geophys. Res. Lett.* **34** L17403
- [38] Estes L D, Beukes H, Bradley B A, Debats S R, Oppenheimer M, Ruane A C, Schulze R and Tadross M 2013 Projected climate impacts to South African maize and wheat production in 2055: a comparison of empirical and mechanistic modeling approaches *Glob. Change Biol.* **19** 3762–74
- [39] Estes L D, Bradley B A, Beukes H, Hole D G, Lau M, Oppenheimer M G, Schulze R, Tadross M A and Turner W R 2013 Comparing mechanistic and empirical model projections of crop suitability and productivity: implications for ecological forecasting *Glob. Ecol. and Biogeogr.* **22** 1007–18
- [40] Mittler R 2006 Abiotic stress, the field environment and stress combination *Trends Plant Sci.* **11** 15–19
- [41] Lobell D B, Hammer G L, McLean G, Messina C, Roberts M J and Schlenker W 2013 The critical role of extreme heat for maize production in the United States *Nat. Clim. Change* **3** 497–501
- [42] Reynolds C 2013 *Foreign agricultural service: Commodity intelligencereport. Tech. rep.* (Washington, DC: United States Department of Agriculture)
- [43] Mahmood R, Foster S A, Keeling T, Hubbard K G, Carlson C and Leeper R 2006 Impacts of irrigation on 20th century temperature in the northern Great Plains *Glob. Planet. Change* **54** 1–18
- [44] Ramankutty N, Foley J A and Olejniczak N J 2002 People on the land: Changes in global population and croplands during the 20th century *AMBIO: J. Human Environ.* **31** 251–7
- [45] Hansen M C *et al* 2013 High-resolution global maps of 21st-century forest cover change *Science* **342** 850–3
- [46] DeFries R, Rudel T, Uriarte M and Hansen M 2010 Deforestation driven by urban population growth and agricultural trade in the twenty-first century *Nat. Geosci.* **3** 178–81
- [47] Niedertscheider M, Gingrich S and Erb K-H 2012 Changes in land use in South Africa between 1961 and 2006: an integrated socio-ecological analysis based on the human appropriation of net primary production framework *Reg. Environ. Change* **12** 715–27
- [48] Moody E G, King M D, Schaaf C B and Platnick S 2008 MODIS-Derived spatially complete surface albedo products: spatial and temporal pixel distribution and zonal averages *J. Appl. Meteorol. Climatol.* **47** 2879–94
- [49] Wild M 2012 Enlightening global dimming and brightening *Bull. Am. Meteorol. Soc.* **93** 27–37
- [50] Streets D G, Wu Y and Chin M 2006 Two-decadal aerosol trends as a likely explanation of the global dimming/brightening transition *Geophys. Res. Lett.* **33** L15806